

Design, synthesis and anticancer activity of naphthoquinone derivatives

Xiao-bao Shen^{a,b}, Yang Wang^a, Xuan-zhen Han^b, Liang-quan Sheng^b, Fu-fang Wu^{a,b} and Xinhua Liu^a

^aSchool of Pharmacy, Anhui Medical University, Hefei, PR China; ^bEngineering Research Center of Biomass Conversion and Pollution Prevention of Anhui Educational Institutions, Fuyang Normal University, Fuyang, PR China

ABSTRACT

Basis on molecular docking and pharmacophore analysis of naphthoquinone moiety, a total of 23 compounds were designed and synthesised. With the help of reverse targets searching, anti-cancer activity was preliminarily evaluated, most of them are effective against some tumour cells, especially compound **12**: 1-(5,8-dihydroxy-1,4-dioxo-1,4-dihydronaphthalen-2-yl)-4-methylpent-3-en-1-yl-4-oxo-4-((4-phenoxyphenyl)amino) butanoate whose IC_{50} against SGC-7901 was $4.1 \pm 2.6 \mu\text{M}$. Meanwhile the anticancer mechanism of compound **12** had been investigated by AnnexinV/PI staining, immunofluorescence, Western blot assay and molecular docking. The results indicated that this compound might induce cell apoptosis and cell autophagy through regulating the PI3K signal pathway.

ARTICLE HISTORY

Received 5 December 2019
Revised 9 February 2020
Accepted 2 March 2020

KEYWORDS

Naphthoquinone moiety;
anticancer activity;
autophagy

1. Introduction

Gastric cancer (GC) is a severe malignant tumour associated with high mortality, especially in Asia^{1,2}. Due to the non-specific symptoms in early appearance and the poor prognosis, the 5-year relative survival rate for GC was at most 20%³. Because of GC difficult diagnosis and chemotherapy resistance, it is necessary to investigate the new therapeutic drugs and deeply explore its anti-tumour mechanism⁴.

Autophagy is a pathway participated in the degradation of lysosomal, which contributed to renew the needed energy of cell survival during starvation^{5,6} and plays an important role in GC. Autophagy is expected to be a new target for molecular therapy⁷ which can inhibit the generation of tumour, on the other hand, can promote the survival and transfer of tumour cells⁸. A large number of studies have shown that autophagy is closely related to DC. For example, the gene polymorphism of autophagy related to the susceptibility of GC^{9,10}. Since lots of compounds regulating autophagy are discovered, but, the tumour microenvironments are complexity, the role of it in the tumour cells is not very clear. Therefore, it is necessary to reveal the title compounds' anticancer mechanism through rational regulating of autophagy.

Compounds with naphthoquinone moiety show good activity against breast cancer, liver cancer, human cervical carcinoma and GC^{11–14} through inducing cell apoptosis^{15–21}. Inducing autophagy is also one of the main mechanisms for anti-cancer activity^{13,22,23}. Among them, PI3K and mTOR signalling pathways have been proved to be the main signal pathways to regulate autophagy^{24–27}. However, for these kinds of derivatives, the poor selectivity and high cytotoxicity limit their clinical application. Therefore, how to reduce the toxicity and increase the selectivity is the main trend. Because the hydroxyl group of naphthoquinone is easily oxidised, and the polyhydroxy is not conducive to selectivity, so modification of the hydroxyl group is one of the main methods to

study structure–activity relationship. Many reports showed that the introduction of suitable substituents on the hydroxyl group could improve activity^{28–30} and reduce toxicity³¹. Furthermore, Ahn³² and Sankawa³³ showed that the side chain hydroxyl was not essential for activity. Both acylation and etherification could maintain antitumor activity at low concentration and the introduction of double bond should increase the activity obviously.

So, based on the above, combined with the results of reverse target finding, a series of new naphthoquinone-esterification/etherification derivatives targeting PI3K were designed and synthesised (Figure 1). Their inhibitory activities against SGC-7901, MGC-803, SMMC-7721, and U-87 cells were determined by MTT assay. The molecular mechanism of title compound was studied by influencing the signal pathway of PI3K/AKT/mTOR. Meanwhile molecular docking was used to determine the interaction between the compound and PI3K protein.

2. Experimental section

2.1. Chemistry

Adriamycin was purchased from Aladdin Chemical Reagent Co., Ltd (Shanghai, China) and other reagents were purchased from Abcam, Cell Signalling Technology (Boston, MA) and Beyotime (Shanghai, China). ¹H NMR spectra were recorded on 400 MHz or 600 MHz and ¹³C NMR spectra were obtained at 100 MHz or 150 MHz (Supplementary material).

2.1.1. General procedure for preparation of compounds 1 and 2

To a solution of shikonin in DMF was added iodomethane (CH₃I, 2.0 equiv) orbenzyl bromide and K₂CO₃ (2.0 equiv) and the mixture was stirred at 60 °C for 6 h. The mixture was filtered and the residue was washed with EA, the filtrate was extracted by EA and

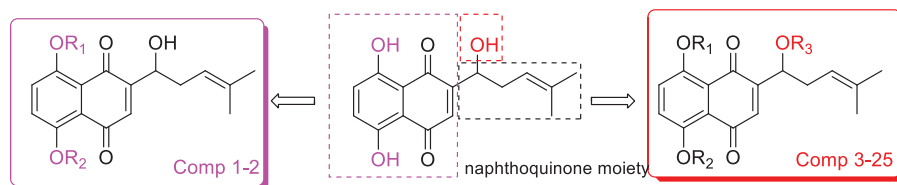


Figure 1. The general design strategy in this study.

combined organic layers were washed with water and brine. Evaporate the solvent and the products were purified by column chromatography to give product as a solid.

1: *2-(1-hydroxy-4-methylpent-3-en-1-yl)-5,8-dimethoxynaphthalene-1,4-dione*, Brown solid. Yield: 92.3%. m.p. 94.3 °C. ¹H NMR (600 MHz, CDCl₃) δ = 7.30 (s, 2H), 6.79 (s, 1H), 5.18–5.13 (m, 1H), 4.77–4.72 (m, 1H), 3.95 (s, 6H), 2.62–2.54 (m, 1H), 2.50 (s, 1H), 2.39–2.33 (m, J = 14.7, 7.5, 1H), 1.71 (s, 3H), 1.61 (s, 32H).

2: *5,8-bis(benzyloxy)-2-(1-hydroxy-4-methylpent-3-en-1-yl)naphthalene-1,4-dione*, Deep red solid. Yield: 37.6%. m.p. 60.0 °C. ¹H NMR (600 MHz, CDCl₃) δ = 12.57 (s, 1H), 12.42 (s, 1H), 7.31–7.17 (m, 7H), 6.86 (s, 1H), 6.02 (dd, J = 6.7, 4.9, 1H), 5.06 (t, J = 7.2, 1H), 2.97 (t, J = 7.7, 2H), 2.79–2.67 (m, 2H), 2.62–2.54 (m, 1H), 2.48–2.42 (m, 1H), 1.67 (s, 3H), 1.56 (s, 3H). ¹³C NMR (150 MHz, CDCl₃) δ 178.18, 176.68, 171.69, 167.39, 166.87, 148.11, 140.04, 136.08, 132.85, 132.68, 131.46, 128.56, 128.21, 126.43, 117.62, 111.78, 111.53, 69.48, 35.75, 32.83, 30.80, 25.76, 17.95. HR-ESI-MS: *m/z* [M + H]⁺ calcd for 469.2064

2.1.2. General procedure for preparation of compounds 3–24

To a solution of amine (1 equiv) in toluene (dichloromethane or furanidine according the amine's solubility) was added succinic anhydride (1.1 equiv) or maleic anhydride (1.1 equiv). Then the solution was refluxed for 0.5 h. After TLC shows the reaction was completed, the solvent was cooled to room temperature. After filtration, cooled toluene was used washing the precipitate to give the crude product, if the product was dissolved in the solvent, the solvent was then removed under reduced pressure to crude product for next step directly.

At 0 °C, dicyclohexyl carbodiimide and 4-dimethylaminopyridine (DMAP) were added and stirred in the solution of above-mentioned carboxylic acid and dichloromethane (DCM) for about 15 min. Then solution of shikonin in DCM was dropped, the combined solution was stirred in ice bath for 6 h, slowly to room temperature. After TLC showed the reaction was completed, the solution was concentrated and cooled to –10 °C and filtered to removal most of the dicyclohexylurea (DCU), the filtrate was evaporated, the product was purified via prepared TLC to give deep red solid.

3: *1-(5,8-dihydroxy-1,4-dioxo-1,4-dihydronaphthalen-2-yl)-4-methylpent-3-en-1-yl-3-phenylpropanoate*, deep red solid. Yield: 37.6%. m.p. 60.0 °C. ¹H NMR (600 MHz, CDCl₃) δ = 12.57 (s, 1H), 12.42 (s, 1H), 7.31–7.17 (m, 7H), 6.86 (s, 1H), 6.02 (dd, J = 6.7, 4.9, 1H), 5.06 (t, J = 7.2, 1H), 2.97 (t, J = 7.7, 2H), 2.79–2.67 (m, 2H), 2.62–2.54 (m, 1H), 2.48–2.42 (m, 1H), 1.67 (s, 3H), 1.56 (s, 3H). ¹³C NMR (150 MHz, CDCl₃) δ 178.18, 176.68, 171.69, 167.39, 166.87, 148.11, 140.04, 136.08, 132.85, 132.68, 131.46, 128.56, 128.21, 126.43, 117.62, 111.78, 111.53, 69.48, 35.75, 32.83, 30.80, 25.76, 17.95. HR-ESI-MS: *m/z* [M + H]⁺ calcd for 421.1632.

4: *1-(5,8-dihydroxy-1,4-dioxo-1,4-dihydronaphthalen-2-yl)-4-methylpent-3-en-1-yl cinnamate*, red solid. Yield: 64.6%. m.p. 85.0 °C. ¹H NMR (600 MHz, CDCl₃) δ = 12.61 (s, 1H), 12.50 (s, 1H), 7.75 (d, J = 16.3, 1H), 7.73–7.70 (m, 1H), 7.54–7.50 (m, 2H), 7.44–7.39 (m, 2H), 7.21–7.16 (m, 3H), 6.45 (d, J = 16.2, 1H), 5.23–5.19 (m, 1H),

4.94–4.91 (m, 1H), 2.68–2.62 (m, 1H), 2.39–2.33 (m, 1H), 1.76 (s, 3H), 1.66 (s, 3H). ¹³C NMR (150 MHz, CDCl₃) δ 180.74, 179.95, 167.72, 165.38, 164.77, 153.99, 151.40, 137.52, 132.42, 132.27, 131.83, 130.91, 128.81, 128.26, 118.39, 112.02, 111.54, 103.67, 65.57, 35.67, 25.97, 18.09. HR-ESI-MS: *m/z* [M + H]⁺ calcd for 419.1482.

5: *1-(5,8-dihydroxy-1,4-dioxo-1,4-dihydronaphthalen-2-yl)-4-methylpent-3-en-1-yl (E)-4-(3,4,5-trimethoxyphenyl)but-3-enoate*, red solid. Yield: 42.5%. m.p. 54.0 °C. ¹H NMR (600 MHz, CDCl₃) δ = 12.60 (s, 1H), 12.41 (s, 1H), 7.62 (d, J = 15.9, 1H), 7.17 (s, 2H), 7.04 (s, 1H), 6.76 (s, 2H), 6.39 (d, J = 15.9, 1H), 6.14–6.11 (m, 1H), 5.16 (t, J = 6.8, 1H), 3.89 (s, 6H), 3.87 (s, 3H), 1.67 (s, 3H), 1.57 (s, 3H). ¹³C NMR (150 MHz, CDCl₃) δ 178.16, 176.67, 167.51, 166.98, 165.60, 153.42, 148.24, 145.89, 140.33, 136.08, 132.88, 132.74, 131.50, 129.56, 117.69, 116.45, 111.82, 111.56, 105.33, 69.60, 60.96, 56.16, 32.90, 25.77, 18.00, 11.20. HR-ESI-MS: *m/z* [M + H]⁺ calcd for 523.1964.

6: *1-(5,8-dihydroxy-1,4-dioxo-1,4-dihydronaphthalen-2-yl)-4-methylpent-3-en-1-yl-2-(4-chlorophenoxy)acetate*, deep red solid. Yield: 85.2%. m.p. 102.0 °C. ¹H NMR (600 MHz, CDCl₃) δ = 12.57 (s, 1H), 12.39 (s, 1H), 7.26–7.22 (m, J = 10.1, 2H), 7.19–7.16 (m, 2H), 6.93 (s, 1H), 6.84 (d, J = 8.9, 2H), 6.15 (dd, J = 7.2, 4.7, 1H), 5.03 (t, J = 7.2, 1H), 4.68 (s, 2H), 2.66–2.60 (m, 1H), 2.51–2.47 (m, 1H), 1.67 (s, 3H), 1.56 (s, 3H). ¹³C NMR (150 MHz, CDCl₃) δ 176.20, 174.62, 169.24, 168.73, 167.64, 156.20, 146.63, 136.59, 133.56, 133.35, 131.17, 129.54, 126.93, 117.14, 115.86, 111.75, 111.53, 70.53, 65.40, 32.76, 25.76, 17.95. HR-ESI-MS: *m/z* [M + H]⁺ calcd for 457.1032.

7: *1-(5,8-dihydroxy-1,4-dioxo-1,4-dihydronaphthalen-2-yl)-4-methylpent-3-en-1-yl-4-oxo-4-(piperidin-1-yl)butanoate*, red solid. Yield: 65.2%. m.p. 120.0 °C. ¹H NMR (600 MHz, CDCl₃) δ = 12.56 (s, 1H), 12.43 (s, 1H), 7.19–7.14 (m, 2H), 7.06 (s, 1H), 6.03–5.98 (m, 1H), 5.16–5.08 (m, 1H), 3.57–3.47 (m, 2H), 3.42–3.33 (m, 2H), 2.73 (t, J = 6.4, 2H), 2.66–2.57 (m, J = 18.5, 11.9, 3H), 2.52–2.44 (m, 1H), 1.67 (s, 3H), 1.64–1.60 (m, J = 4.3, 2H), 1.57–1.48 (m, 7H). ¹³C NMR (150 MHz, CDCl₃) δ 194.47, 178.95, 177.49, 172.20, 168.93, 166.70, 166.18, 148.19, 135.96, 132.58, 132.35, 131.97, 117.71, 111.57, 69.62, 65.57, 46.29, 42.87, 32.77, 29.41, 27.92, 26.32, 25.77, 24.48, 17.96. HR-ESI-MS: *m/z* [M + H]⁺ calcd for 456.2042.

8: *1-(5,8-dihydroxy-1,4-dioxo-1,4-dihydronaphthalen-2-yl)-4-methylpent-3-en-1-yl 4-morpholino-4-oxobutanoate*, red solid. Yield: 26.4%. m.p. 105.0 °C. ¹H NMR (600 MHz, CDCl₃) δ = 12.56 (s, 1H), 12.43 (s, 1H), 7.19–7.14 (m, 2H), 7.05 (s, 1H), 6.01 (dd, J = 6.3, 5.3, 1H), 5.12 (t, J = 7.2, 1H), 3.68–3.63 (m, 4H), 3.61–3.58 (m, 2H), 3.48–3.45 (m, 2H), 2.75 (t, J = 6.6, 2H), 2.67–2.58 (m, 3H), 2.53–2.43 (m, 1H), 1.68 (s, 3H), 1.56 (s, 3H). ¹³C NMR (150 MHz, CDCl₃) δ 178.62, 177.13, 172.00, 169.50, 167.02, 166.50, 148.01, 136.03, 132.71, 132.49, 131.85, 117.65, 111.80, 111.56, 69.77, 66.83, 66.46, 45.61, 42.06, 32.76, 29.17, 27.71, 25.78, 17.96. HR-ESI-MS: *m/z* [M + H]⁺ calcd for 458.1831.

9: *1-(5,8-dihydroxy-1,4-dioxo-1,4-dihydronaphthalen-2-yl)-4-methylpent-3-en-1-yl-4-(3,4-dihydroquinolin-1(2H)-yl)-4-oxobutanoate*, red solid. Yield: 44.1%. m.p. 92.0 °C. ¹H NMR (600 MHz, CDCl₃) δ = 12.57 (s, 1H), 12.44 (s, 1H), 7.19–7.07 (m, 6H), 7.05 (s, 1H), 6.02–5.98 (m, 1H), 5.11 (t, J = 7.0, 1H), 3.83–3.73 (m, 2H), 2.82–2.78 (m, 2H), 2.77–2.75 (m, 2H), 2.72–2.69 (m, 2H), 2.64–2.58 (m, 1H),

2.52–2.45 (m, 1H), 1.98–1.88 (m, 2H), 1.67 (s, 3H), 1.55 (s, 3H). ¹³C NMR (150 MHz, CDCl₃) δ 178.72, 177.25, 171.93, 166.89, 166.38, 156.74, 148.11, 136.00, 132.65, 132.43, 131.88, 128.54, 126.10, 124.68, 117.66, 111.80, 111.56, 69.69, 49.12, 33.92, 32.77, 29.62, 26.77, 25.76, 25.59, 24.93, 23.96, 17.95. HR-ESI-MS: *m/z* [M + H]⁺ calcd for 504.2024.

10: 1-(5,8-dihydroxy-1,4-dioxo-1,4-dihydronaphthalen-2-yl)-4-methylpent-3-en-1-yl-4-((4-methoxyphenyl)amino)-4-oxobutanoate, red solid. Yield: 72.9%. m.p. 115.0 °C. ¹H NMR (600 MHz, CDCl₃) δ = 12.57 (s, 1H), 12.41 (s, 1H), 7.36 (d, *J* = 8.8, 2H), 7.34 (s, 1H), 7.19–7.15 (m, 2H), 7.04 (s, 1H), 6.82 (d, *J* = 8.8, 2H), 6.04 (dd, *J* = 6.4, 5.3, 1H), 5.11 (t, *J* = 7.0, 1H), 3.77 (s, 3H), 2.83 (t, *J* = 6.6, 2H), 2.65 (t, *J* = 6.5, 2H), 2.62–2.58 (m, 1H), 2.52–2.46 (m, 1H), 1.66 (s, 3H), 1.56 (s, 3H). ¹³C NMR (150 MHz, CDCl₃) δ 207.18, 177.88, 176.40, 172.17, 169.21, 168.00, 167.47, 156.52, 147.82, 136.41, 133.16, 132.93, 131.79, 130.96, 121.70, 117.65, 114.23, 111.96, 111.72, 70.15, 55.60, 32.96, 31.98, 31.09, 29.73, 25.90, 18.11. HR-ESI-MS: *m/z* [M + H]⁺ calcd for 494.1839.

11: 1-(5,8-dihydroxy-1,4-dioxo-1,4-dihydronaphthalen-2-yl)-4-methylpent-3-en-1-yl-4-((4-fluoro-3-(trifluoromethyl)phenyl)amino)-4-oxobutanoate, red solid. Yield: 63.2%. m.p. 137.0 °C. ¹H NMR (600 MHz, CDCl₃) δ = 12.56 (s, 1H), 12.39 (s, 1H), 7.76–7.72 (m, 1H), 7.70–7.63 (m, 2H), 7.19–7.13 (m, 2H), 7.11 (t, *J* = 9.3, 1H), 7.03 (s, 1H), 6.07–6.02 (m, 1H), 5.10 (t, *J* = 6.9, 1H), 2.85–2.81 (m, 2H), 2.69–2.58 (m, 3H), 2.52–2.45 (m, 1H), 1.65 (s, 3H), 1.56 (s, 3H). ¹³C NMR (150 MHz, CDCl₃) δ 207.09, 177.19, 175.67, 172.03, 169.54, 168.32, 167.80, 147.36, 136.32, 136.29, 133.89, 133.20, 132.96, 131.44, 124.85, 118.30, 117.39, 117.22, 111.76, 111.51, 70.21, 32.78, 31.78, 30.92, 29.30, 25.71, 17.93. HR-ESI-MS: *m/z* [M + H]⁺ calcd for 550.1437.

12: 1-(5,8-dihydroxy-1,4-dioxo-1,4-dihydronaphthalen-2-yl)-4-methylpent-3-en-1-yl-4-oxo-4-((4-phenoxyphenyl)amino)butanoate, red solid. Yield: 82.1%. m.p. 133.0 °C. ¹H NMR (600 MHz, CDCl₃) δ = 12.59–12.55 (m, 1H), 12.40 (s, 1H), 7.47–7.38 (m, 3H), 7.30 (t, *J* = 7.8, 2H), 7.19–7.13 (m, 2H), 7.07 (t, *J* = 7.4, 1H), 7.04 (s, 1H), 6.95 (t, *J* = 9.5, 4H), 6.06–6.02 (m, 1H), 5.10 (t, *J* = 7.2, 1H), 2.84 (t, *J* = 6.5, 2H), 2.66 (t, *J* = 6.5, 2H), 2.64–2.57 (m, 1H), 2.49–2.42 (m, 1H), 1.66 (s, 3H), 1.56 (s, 3H). ¹³C NMR (150 MHz, CDCl₃) δ 177.60, 176.09, 172.01, 169.20, 167.94, 167.42, 153.39, 147.59, 136.26, 133.21, 133.05, 132.82, 131.57, 129.68, 123.02, 121.42, 119.57, 118.36, 117.46, 111.78, 111.55, 70.04, 32.80, 31.83, 29.48, 25.73, 17.95. HR-ESI-MS: *m/z* [M + H]⁺ calcd for 556.1958.

13: 1-(5,8-dihydroxy-1,4-dioxo-1,4-dihydronaphthalen-2-yl)-4-methylpent-3-en-1-yl-4-oxo-4-((4-(trifluoromethoxy)phenyl)amino)butanoate, red solid. Yield: 58.6%. m.p. 134.0 °C. ¹H NMR (600 MHz, CDCl₃) δ = 12.56 (s, 1H), 12.40 (s, 1H), 7.56 (br, 1H), 7.50 (d, *J* = 8.7, 2H), 7.18–7.11 (m, 4H), 7.04 (s, 1H), 6.05–6.02 (m, 1H), 5.10 (t, *J* = 7.0, 1H), 2.83 (t, *J* = 6.4, 2H), 2.67 (t, *J* = 6.3, 2H), 2.64–2.58 (m, 1H), 2.52–2.45 (m, 1H), 1.65 (s, 3H), 1.55 (s, 3H). ¹³C NMR (150 MHz, CDCl₃) δ 177.38, 175.87, 171.99, 169.27, 168.15, 167.62, 147.45, 136.75, 136.29, 133.14, 132.89, 131.88, 131.53, 121.13, 117.42, 116.79, 111.76, 111.54, 70.12, 32.78, 32.00, 30.92, 29.41, 25.73, 17.94. HR-ESI-MS: *m/z* [M + H]⁺ calcd for 548.1546.

14: 1-(5,8-dihydroxy-1,4-dioxo-1,4-dihydronaphthalen-2-yl)-4-methylpent-3-en-1-yl-4-((4-bromophenyl)amino)-4-oxobutanoate, red solid. Yield: 77.6%. m.p. 105.0 °C. ¹H NMR (600 MHz, CDCl₃) δ = 12.56 (s, 1H), 12.40 (s, 1H), 7.47 (br, 1H), 7.40–7.33 (m, 4H), 7.19–7.14 (m, 2H), 7.03 (s, 1H), 6.06–6.01 (m, 1H), 5.09 (t, *J* = 7.2, 1H), 2.82 (t, *J* = 6.4, 2H), 2.68–2.57 (m, 3H), 2.53–2.44 (m, 1H), 1.65 (s, 3H), 1.55 (s, 3H). ¹³C NMR (150 MHz, CDCl₃) δ 177.38, 175.87, 171.99, 169.27, 168.15, 167.62, 147.45, 136.75, 136.29, 133.14, 132.89, 131.88, 131.53, 121.13, 117.42, 116.79, 111.76, 111.54,

70.12, 32.78, 32.00, 30.92, 29.41, 25.73, 17.94. HR-ESI-MS: *m/z* [M + H]⁺ calcd for 542.0732.

15: 1-(5,8-dihydroxy-1,4-dioxo-1,4-dihydronaphthalen-2-yl)-4-methylpent-3-en-1-yl-4-((2-methoxyphenyl)amino)-4-oxobutanoate, red solid. Yield: 87.3%. m.p. 113.0 °C. ¹H NMR (600 MHz, CDCl₃) δ = 12.57 (s, 1H), 12.42 (s, 1H), 8.32 (d, *J* = 7.8, 1H), 7.85 (br, 1H), 7.18–7.14 (m, 2H), 7.05–7.04 (m, 1H), 7.02–6.98 (m, 1H), 6.95–6.91 (m, 1H), 6.83 (d, *J* = 8.2, 1H), 6.05–6.02 (m, 1H), 5.13–5.08 (m, 1H), 3.85 (s, 3H), 2.83 (t, *J* = 6.6, 2H), 2.72 (t, *J* = 6.5, 2H), 2.64–2.57 (m, 1H), 2.51–2.45 (m, 1H), 1.66 (s, 3H), 1.55 (s, 3H). ¹³C NMR (150 MHz, CDCl₃) δ 207.02, 177.72, 176.24, 172.01, 169.05, 167.84, 167.31, 156.36, 147.66, 136.25, 133.00, 132.77, 131.63, 130.80, 121.54, 117.49, 114.07, 111.74, 111.56, 69.99, 55.44, 32.80, 31.82, 30.93, 29.57, 25.74, 17.95. HR-ESI-MS: *m/z* [M + H]⁺ calcd for 494.1853.

16: 1-(5,8-dihydroxy-1,4-dioxo-1,4-dihydronaphthalen-2-yl)-4-methylpent-3-en-1-yl-4-(naphthalen-1-ylamino)-4-oxobutanoate, red solid. Yield: 74.8%. m.p. 127.0 °C. ¹H NMR (600 MHz, CDCl₃) δ = 12.54 (s, 1H), 12.26 (s, 1H), 7.94 (d, *J* = 7.1, 1H), 7.89 (br, 1H), 7.82–7.76 (m, 2H), 7.64 (d, *J* = 8.2, 1H), 7.47–7.37 (m, 3H), 7.17–7.10 (m, 2H), 6.97 (s, 1H), 6.11–6.04 (m, 1H), 5.14–5.05 (m, 1H), 2.93 (t, *J* = 5.5, 2H), 2.87–2.79 (m, 1H), 2.63–2.57 (m, 2H), 2.51–2.43 (m, 1H), 1.63 (s, 3H), 1.54 (s, 3H). ¹³C NMR (150 MHz, CDCl₃) δ 177.20, 172.38, 169.95, 167.43, 156.69, 147.43, 136.30, 133.90, 133.00, 132.72, 132.06, 131.41, 130.89, 128.81, 128.65, 126.66, 126.15, 125.85, 125.70, 125.63, 120.45, 117.43, 111.73, 70.18, 33.92, 32.77, 25.58, 24.91, 17.93. HR-ESI-MS: *m/z* [M + H]⁺ calcd for 514.1846.

17: 1-(5,8-dihydroxy-1,4-dioxo-1,4-dihydronaphthalen-2-yl)-4-methylpent-3-en-1-yl-4-((3-chlorophenethyl)amino)-4-oxobutanoate, red solid. Yield: 46.3%. m.p. 91.8 °C. ¹H NMR (600 MHz, CDCl₃) δ = 12.57 (s, 1H), 12.41 (s, 1H), 7.23–7.14 (m, 5H), 7.05 (d, *J* = 7.2, 1H), 7.00 (s, 1H), 6.01 (dd, *J* = 6.3, 5.1, 1H), 5.61 (s, 1H), 5.10 (t, *J* = 7.3, 1H), 3.49–3.42 (m, 2H), 2.77–2.72 (m, 4H), 2.62–2.54 (m, 1H), 2.48–2.38 (m, 3H), 1.67 (s, 3H), 1.56 (s, 3H). ¹³C NMR (150 MHz, CDCl₃) δ 177.84, 176.33, 171.85, 171.02, 167.74, 167.20, 147.82, 140.82, 136.17, 134.34, 132.97, 132.74, 131.54, 129.84, 128.85, 126.91, 126.71, 117.53, 111.78, 111.54, 69.86, 40.53, 35.29, 32.81, 30.81, 29.44, 25.76, 17.95. HR-ESI-MS: *m/z* [M + H]⁺ calcd for 526.1632.

18: 1-(5,8-dihydroxy-1,4-dioxo-1,4-dihydronaphthalen-2-yl)-4-methylpent-3-en-1-yl-4-((2-chlorophenethyl)amino)-4-oxobutanoate, red solid. Yield: 76.6%. m.p. 97.8 °C. ¹H NMR (600 MHz, CDCl₃) δ = 12.57 (s, 1H), 12.41 (s, 1H), 7.34–7.32 (m, 1H), 7.20–7.14 (m, 5H), 7.01 (s, 1H), 6.01 (dd, *J* = 6.5, 5.2, 1H), 5.62 (s, 1H), 5.10 (t, *J* = 7.3, 1H), 3.51 (dd, *J* = 13.2, 6.8, 2H), 2.92 (t, *J* = 7.0, 2H), 2.79–2.70 (m, 2H), 2.64–2.58 (m, 1H), 2.50–2.41 (m, 3H), 1.68 (s, 3H), 1.56 (s, 3H). ¹³C NMR (150 MHz, cdcl₃) δ 177.85, 176.34, 171.84, 170.98, 167.73, 167.20, 147.84, 136.45, 136.17, 134.07, 132.96, 132.73, 131.55, 131.00, 129.59, 128.04, 126.97, 117.54, 111.79, 111.55, 69.81, 39.28, 33.29, 32.82, 30.81, 29.44, 25.76, 17.95. HR-ESI-MS: *m/z* [M + H]⁺ calcd for 526.1662.

19: 1-(5,8-dihydroxy-1,4-dioxo-1,4-dihydronaphthalen-2-yl)-4-methylpent-3-en-1-yl-4-((4-bromophenethyl)amino)-4-oxobutanoate, red solid. Yield: 69.4%. m.p. 134.0 °C. ¹H NMR (600 MHz, CDCl₃) δ = 12.58 (s, 1H), 12.41 (s, 1H), 7.40 (d, *J* = 8.2, 2H), 7.16 (s, 2H), 7.04 (d, *J* = 8.2, 2H), 7.00 (s, 1H), 6.06–5.95 (m, 1H), 5.58 (s, 1H), 5.10 (t, *J* = 7.1, 1H), 3.49–3.43 (m, 2H), 2.77–2.70 (m, 4H), 2.61–2.56 (m, 1H), 2.52–2.47 (m, 1H), 2.42 (t, *J* = 6.7, 2H), 1.67 (s, 3H), 1.56 (s, 3H). ¹³C NMR (150 MHz, CDCl₃) δ 177.77, 176.25, 171.85, 170.99, 167.81, 167.28, 147.80, 137.72, 136.18, 132.99, 132.78, 131.65, 131.51, 130.46, 120.35, 117.52, 111.78, 111.54, 69.85, 40.55, 35.05,

33.92, 32.81, 30.79, 29.42, 25.76, 25.58, 17.95. HR-ESI-MS: m/z $[M + H]^+$ calcd for 570.1137.

20: 1-(5,8-dihydroxy-1,4-dioxo-1,4-dihydronaphthalen-2-yl)-4-methylpent-3-en-1-yl 4-((4-fluorophenethyl)amino)-4-oxobutanoate, red solid. Yield: 54.2%. m.p. 116.0 °C. 1H NMR (600 MHz, $CDCl_3$) δ = 12.57 (s, 1H), 12.41 (s, 1H), 7.16 (s, 2H), 7.14–7.10 (m, 2H), 7.00 (s, 1H), 6.97 (t, J = 8.6, 2H), 6.05–6.00 (m, 1H), 5.59 (br, 1H), 5.10 (t, J = 7.3, 1H), 3.51–3.44 (m, 2H), 2.77–2.70 (m, J = 6.8, 4H), 2.66–2.55 (m, 1H), 2.52–2.45 (m, 1H), 2.42 (t, J = 6.8, 2H), 1.67 (s, 3H), 1.56 (s, 3H). ^{13}C NMR (150 MHz, $CDCl_3$) δ 177.80, 176.28, 171.86, 170.96, 167.78, 167.25, 162.42, 160.79, 147.81, 136.18, 132.98, 132.76, 131.52, 130.13, 130.08, 117.52, 115.45, 115.31, 111.78, 111.54, 69.84, 40.81, 34.82, 32.81, 30.80, 29.44, 25.75, 17.94. HR-ESI-MS: m/z $[M + H]^+$ calcd for 510.1936.

21: 1-(5,8-dihydroxy-1,4-dioxo-1,4-dihydronaphthalen-2-yl)-4-methylpent-3-en-1-yl 4-((2-fluorophenethyl)amino)-4-oxobutanoate, red solid. Yield: 75.5%. m.p. 91.0 °C. 1H NMR (600 MHz, $CDCl_3$) δ = 12.57 (s, 1H), 12.41 (s, 1H), 7.21–7.15 (m, 4H), 7.06 (t, J = 7.4, 1H), 7.03–6.98 (m, 2H), 6.04–5.98 (m, 1H), 5.64 (br, 1H), 5.10 (t, J = 7.2, 1H), 3.49 (q, J = 6.7, 2H), 2.83 (t, J = 6.9, 2H), 2.75–2.69 (m, 2H), 2.64–2.58 (m, 1H), 2.50–2.46 (m, 1H), 2.43 (t, J = 6.9, 2H), 1.67 (s, 3H), 1.56 (s, 3H). ^{13}C NMR (150 MHz, $CDCl_3$) δ 177.92, 176.41, 171.83, 170.98, 167.67, 167.14, 162.03, 160.41, 147.86, 136.16, 132.94, 132.71, 131.56, 131.14, 131.11, 128.35, 128.30, 125.74, 125.63, 124.21, 124.19, 117.55, 115.40, 115.26, 111.79, 111.54, 69.80, 39.67, 32.81, 30.79, 29.45, 29.09, 25.75, 17.94. HR-ESI-MS: m/z $[M + H]^+$ calcd for 510.1966.

22: 1-(5,8-dihydroxy-1,4-dioxo-1,4-dihydronaphthalen-2-yl)-4-methylpent-3-en-1-yl 4-(diethylamino)-4-oxobutanoate, red solid. Yield: 78.5%. m.p. 77.0 °C. 1H NMR (600 MHz, $CDCl_3$) δ = 12.57 (s, 1H), 12.43 (s, 1H), 7.19–7.14 (m, 2H), 7.05 (s, 1H), 6.02–5.99 (m, 1H), 5.12 (t, J = 7.2, 1H), 3.36 (q, J = 7.1, 1H), 3.31 (q, J = 7.1, 2H), 2.75 (t, J = 6.7, 2H), 2.65–2.58 (m, 3H), 2.52–2.47 (m, 1H), 1.67 (s, 3H), 1.56 (s, 3H), 1.18 (t, J = 7.1, 3H), 1.08 (t, J = 7.1, 3H). ^{13}C NMR (150 MHz, $CDCl_3$) δ 178.85, 177.39, 172.17, 169.81, 166.79, 166.27, 148.18, 135.95, 132.60, 132.37, 131.92, 117.70, 111.82, 111.57, 69.65, 41.73, 40.28, 32.78, 29.43, 27.85, 25.75, 17.94, 14.12, 13.04. HR-ESI-MS: m/z $[M + H]^+$ calcd for 444.2024.

23: 1-(5,8-dihydroxy-1,4-dioxo-1,4-dihydronaphthalen-2-yl)-4-methylpent-3-en-1-yl 4-(dihexylamino)-4-oxobutanoate 1-(5,8-dihydroxy-1,4-dioxo-1,4-dihydronaphthalen-2-yl)-4-methylpent-3-en-1-yl 4-(dihexylamino)-4-oxobutanoate, red solid. Yield: 53.8%. m.p. 78.3 °C. 1H NMR (600 MHz, $CDCl_3$) δ = 12.56 (s, 1H), 12.44 (s, 1H), 7.19–7.14 (m, 2H), 7.05 (s, 1H), 6.00 (dd, J = 6.3, 5.0, 1H), 5.12 (t, J = 7.2, 1H), 3.29–3.25 (m, 2H), 3.22–3.18 (m, 2H), 2.74 (t, J = 6.7, 2H), 2.65–2.58 (m, 3H), 2.51–2.45 (m, 1H), 1.67 (s, 3H), 1.55 (s, 3H), 1.32–1.21 (m, 16H), 0.90–0.83 (m, 6H). ^{13}C NMR (150 MHz, $CDCl_3$) δ 178.92, 177.47, 172.18, 170.11, 166.71, 166.19, 148.19, 135.94, 132.58, 132.34, 131.96, 117.71, 111.81, 111.56, 69.62, 47.82, 46.17, 32.78, 31.60, 31.50, 29.69, 29.48, 28.87, 27.90, 27.71, 26.70, 26.60, 25.77, 22.59, 17.95, 14.04, 13.99. HR-ESI-MS: m/z $[M + H]^+$ calcd for 556.3284.

24: 1-(5,8-dihydroxy-1,4-dioxo-1,4-dihydronaphthalen-2-yl)-4-methylpent-3-en-1-yl (Z)-4-morpholino-4-oxobut-2-enoate, red solid. Yield: 49.6%. m.p. 104.0 °C. 1H NMR (600 MHz, $CDCl_3$) δ = 12.57 (s, 1H), 12.40 (s, 1H), 7.17 (s, 2H), 7.02 (s, 1H), 6.61 (d, J = 11.9, 1H), 6.12 (d, J = 11.9, 1H), 6.09 (dd, J = 6.3, 4.9, 1H), 5.10 (t, J = 7.1, 1H), 3.74–3.58 (m, 4H), 2.91 (dd, J = 16.5, 4.5, 2H), 2.76 (dd, J = 16.6, 4.6, 2H), 2.67–2.61 (m, 1H), 2.53–2.45 (m, 1H), 1.67 (s, 3H), 1.55 (s, 3H). ^{13}C NMR (150 MHz, $CDCl_3$) δ = 180.62, 179.13, 174.00, 171.50, 169.02, 168.50, 150.01, 138.03, 137.29, 134.71, 134.49, 133.85, 124.11, 119.65, 113.80, 113.56, 71.77, 68.83, 68.46, 47.61, 44.06, 29.71, 27.78, 19.96. HR-ESI-MS: m/z $[M + H]^+$ calcd for 456.1628.

2.2. Cell culture

MGC-803, SGC-7901, U87 and SMMC-7721 cell lines were cultured in DMEM supplemented with 10% foetal bovine serum, 100 IU/mL penicillin/streptomycin. The cells were incubated in an atmosphere containing 5% CO_2 at 37 °C.

2.3. Cell viability assay

MGC-803, SGC-7901, U87 and SMMC-7721 cells were plated in 96-well plate at 7000 per well. Cells were incubated with the different concentrations of the compounds for 48 h. Subsequently, MTT (0.5 mg/mL) were used to test the cell viability, then 150 μ L DMSO was added to each well after cells were incubated for 4 h and the absorbance was measured at 492 nm.

2.4. Apoptosis assay

After the indicated treatments for 48 h, cells were collected, washed three times with cold PBS, centrifuged and resuspended with 400 μ L AnnexinV binding buffer per tube. Then the cells were stained with 5 μ L AnnexinV-FITC and incubated in the dark for 10 min on ice. Finally, 10 μ L PI staining solution was added, and cells were detected by the flow cytometry after incubated in the dark for 5 min. Flowjo 7.6.1 software was used to analyse the cell apoptosis.

2.5. Colony formation assay

SGC-7901 cells (8000/well) were seeded in 6-well plate, and treated with indicated concentrations of compound **12** (2 μ M, 4 μ M, 8 μ M) for 12 d. The medium was removed and methanol (500 μ L/well) was added to fix at the cells for 3 min. Then cells were stained with giemsa working fluid for 15 min and washed with PBS. The number of colonies was counted.

2.6. Acridineorange (AO) staining

PH-sensitive Acridine orange (AO) was used to label acidic vesicles. Human gastric cancer cells were seeded in laser confocal dishes at 10,000/ml. After indicated treatment of compound **12** (1 μ M, 2 μ M, 4 μ M) for 48 h, cells were stained with AO (1 μ g/ml) for 15 min at the cell culture incubator. After the cells were washed by PBS, pictures were acquired under laser confocal microscope.

2.7. GFP-LC3 transfection

A plasmid GFP-tagged LC3 reporter gene (0.8 μ g/500 μ L) was transfected into SGC-7901 cells by Lipofectamine 2000, then cells were incubated for 24 h. After different treatments for 24 h, cells were fixed with 4% paraformaldehyde for 20 min, and washed three times with PBS. Finally, Laser confocal dishes were analysed using confocal microscope.

2.8. Western blot analysis

RIPA lysis buffer was used to dissociate the treated cells. Cells were lysed and the supernatant was harvested after centrifuged for 30 min. The cell proteins were separated using Sodium dodecyl sulphate-polyacrylamide gel electrophoresis, and then they were transferred to the PVDF membranes. The membranes were

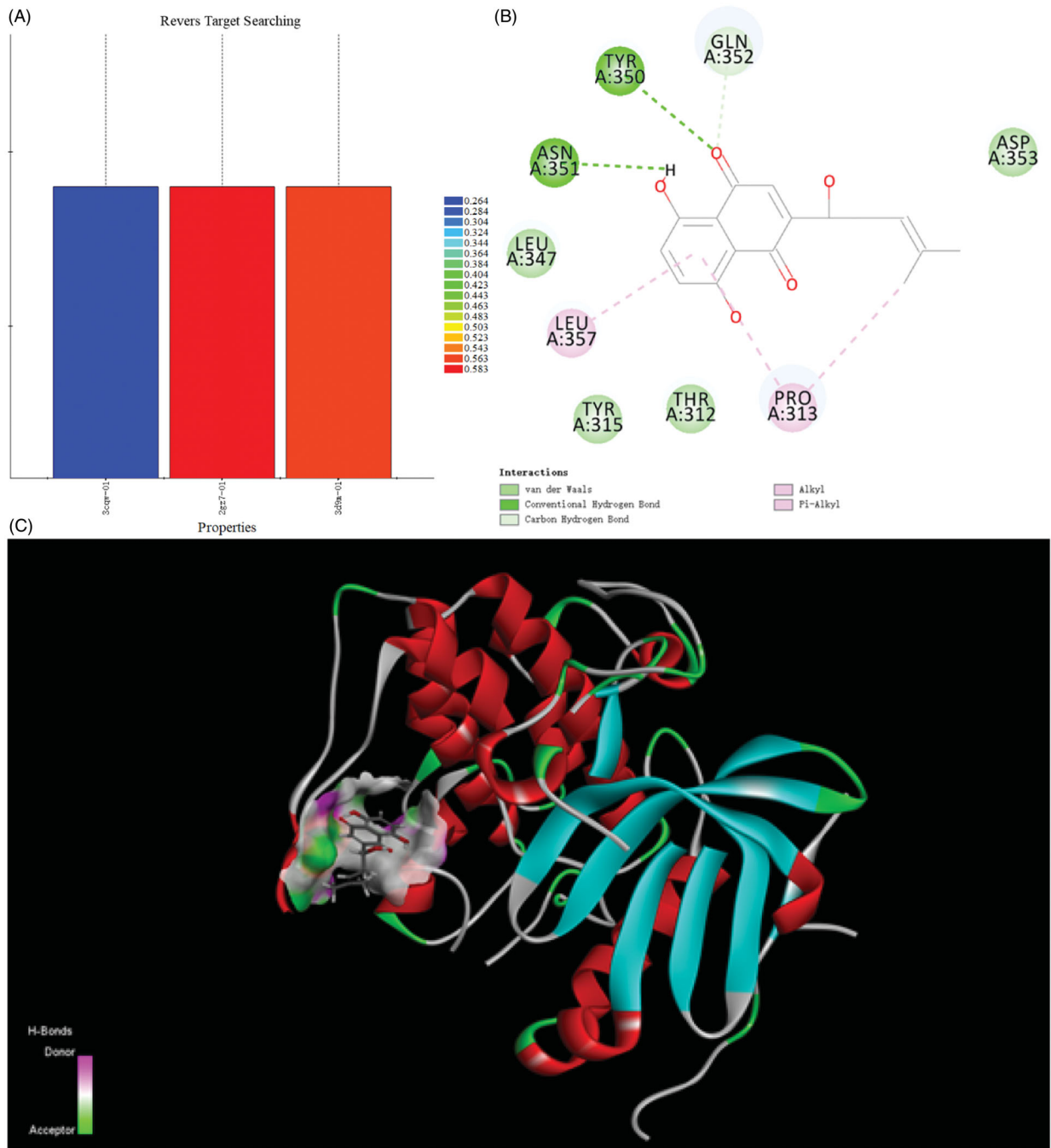


Figure 2. Ligand profiler and docking result of naphthoquinone moiety.

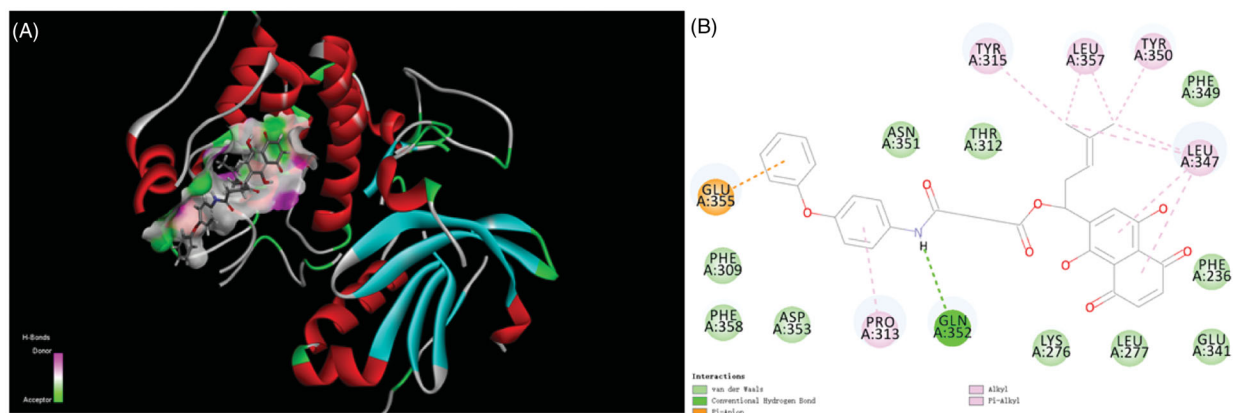
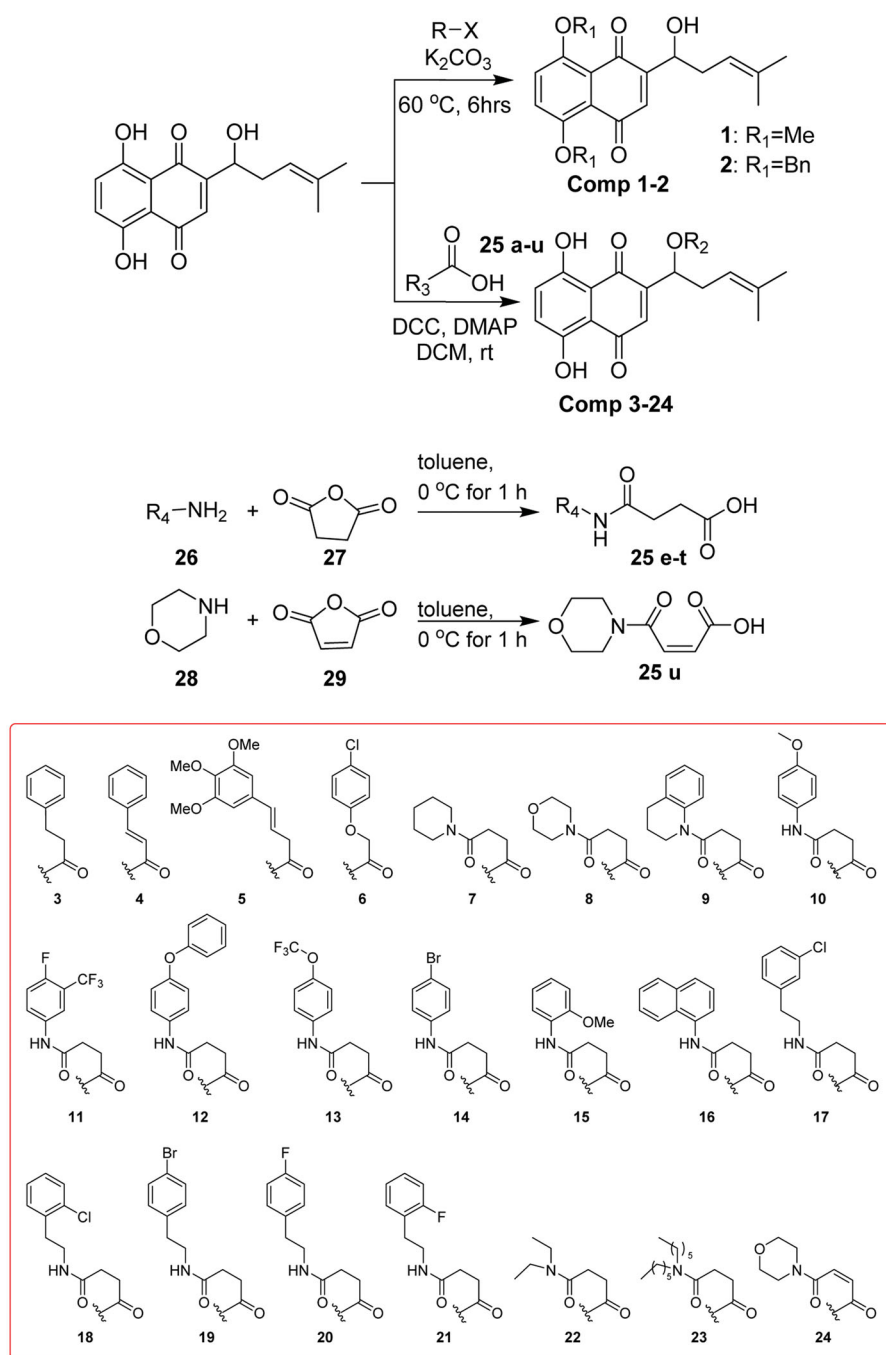


Figure 3. Docking result of compound 12 with Akt.



Scheme 1. Synthesis of title compounds 1–24.

blocked with skimmed milk solution (5%) for 2 h, then incubated with primary antibodies (1:1000, cst) for 20 h at 4 °C. The membranes were detected by chemiluminescence reagent after probed with the secondary antibody for 1 h.

2.9. Statistical analysis

Data were represented as the mean \pm SD (standard deviation). GraphPad Prism 5.0 software (GraphPad Software, La Jolla, CA) were used to analyse significance by one-way ANOVA. $p < 0.05$ was expressed a significant difference.

3. Results

3.1. Scaffold design

Discovery Studio 2018 was used as computation programme and naphthoquinone moiety as ligand to execute reverse targets searching programme, targets were searched to suit the pharmacophores of protein active sites in the database. Comparison with protein data bank, the results indicated the PI3K/Akt signal pathway was the target of naphthoquinone moiety. The lower most CDOCKER energy of all conformations is 6.13917 kcal/m. The moiety interacted with protein active site through those forces, containing van der Waals force, conventional hydrogen bond,

carbon hydrogen bond, alkyl and Pi-alkyl interactions. Van der Waals force formed between naphthoquinone and the receptors (Thr312, Tyr315, Leu347, Gln352). There was a hydrogen bond interaction between Asn351 and compound. Alkyl and Pi-Alkyl interacts with the aryl ring and the alkyl group via Leu357 and Pro313 (Figure 2).

Title compound **12** has five kinds of interactions, such as hydrogen bonds, Pi-Anion force, Pi-alkyl interactions, and conventional van der Waals force which were formed with Phe309, Phe349, Phe358, Asp353, Asn351, Thr312, Lys276, Leu277, Glu341 and Phe236. Between the nitrogen of the compound and Gln352 formed the hydrogen bond. There also existed a Pi-anion interaction between aryl ring and the Glu355. Alky and Pi-Alkyl interactions were formed between aryl rings and Pro313, Tyr315, Leu357, Tyr350 and Leu347. Compared with naphthoquinone moiety, there was more stronger interaction of compound **12** than that of

it. The differences of CDDOCKER energy also proved this. (The lower most CDDOCKER Energy of compound **12** is -15.7597 kcal/m and naphthoquinone is 6.13917 kcal/m). These data indicated that the combination of title compound **12** with the cavity site of Akt (PDB ID:3CQW) is spontaneous, which was more easier than that of naphthoquinone moiety (Figure 3).

3.2. Chemistry

Compounds **1** and **2** can be obtained by substitution of halides with phenol hydroxyls of naphthoquinone. The condensation reaction between hydroxyl group on side-chain of naphthoquinone and the related acids can get compounds **3–24**. Compounds **25e–u** were obtained from succinic anhydride or maleic anhydride after ring-opening reaction (Scheme 1).

3.3. Evaluation of anti-proliferation activity

Compounds **1–24** were detected for anticancer activities against SGC-7901, MGC-803, SMMC-7721, U-87 cell lines *in vitro* by the MTT assay, and ADM was used as the positive control³⁴. From Table 1, when the phenolic hydroxyls of naphthoquinone moiety were converted to ether, the activity was missing. Compounds **9**, **11**, **12**, **13**, **17** and **20** have good activity which showed that hydroxyl group on side-chain of naphthoquinone moiety was modifiable and the introducing of hydrogen-bond donor, acceptor and hydrophobic group could benefit the activity. Compound **12** displayed high activity against the MGC-803, SGC-7901 and U87 cells with the IC_{50} s of 4.07, 4.09 and $3.85 \mu\text{M}$, respectively. So colony formation assay of this compound (Figure 4) was used to investigate the effect of it on cell proliferation in SGC-7901 cells. The experiment examined the ability for producing colonies after the cells were treated with the cell death agents^{35,36}. The results exhibited that the colonies were decreased with the increased concentration of the title compound compared with the control group, which revealed this compound could inhibit the cell proliferation.

3.4. Metabolic stability assay in human liver microsomes

To initially evaluate the stability of compound **12**, we then tested the liver microsome stability of this compound. The Mean %

Table 1. *In vitro* anticancer activities of compounds 1–24 against U 87, SMMC-7721, SGC-7901, MGC-803 cell lines.

Compounds	$IC_{50} \mu\text{M}$ ($n=3$)				
	U87	SMMC-7721	SGC-7901	MGC-803	L02
1	–	–	–	–	– ^a
2	–	–	–	–	–
3	8.0 ± 0.85	15.6 ± 3.3	10.6 ± 4.3	4.5 ± 1.1	13.6 ± 1.5
4	65.7 ± 2.7	–	75.1 ± 0.4	–	–
5	–	–	–	–	–
6	–	–	–	–	–
7	9.68 ± 2.3	14.4 ± 1.5	33.6 ± 2.1	9.7 ± 2.3	36.8 ± 4.1
8	10.0 ± 1.6	16.7 ± 1.8	20 ± 3.9	10.4 ± 0.7	>50
9	4.45 ± 0.66	12.3 ± 0.1	8.6 ± 2.5	3.1 ± 0.1	12.1 ± 0.8
10	12.3 ± 2.8	12.4 ± 2.6	11.1 ± 1.2	7.9 ± 1.8	11.9 ± 0.6
11	3.75 ± 0.77	9.5 ± 0.8	2.25 ± 1.5	8.4 ± 3.1	4.0 ± 0.1
12	3.8 ± 0.2	20.6 ± 0.4	4.1 ± 2.6	4.1 ± 0.6	>50
13	3.46 ± 0.31	16.9 ± 2.2	7.8 ± 3.7	10.2 ± 2.9	15.8 ± 1.1
14	–	14.8 ± 0.1	10.7 ± 1.8	10.2 ± 1.3	16.2 ± 1.7
15	–	–	–	–	–
16	5.41 ± 0.67	24.3 ± 1.7	5.6 ± 2.6	5.9 ± 2.6	13.0 ± 2.4
17	3.8 ± 1.7	15.9 ± 0.2	20.8 ± 0.5	6.7 ± 2.4	11.4 ± 1.8
18	7.7 ± 4.4	17.9 ± 1.6	23.7 ± 0.5	6.6 ± 4.7	20.2 ± 2.0
19	9.1 ± 2.5	17.9 ± 1.0	7.6 ± 2.3	5.7 ± 2.4	8.5 ± 0.4
20	5.2 ± 1.4	18.6 ± 3.6	13.3 ± 0.6	3.5 ± 1.4	12.3 ± 0.5
21	6.1 ± 0.6	15.4 ± 0.4	14.8 ± 1.6	6.9 ± 3.9	16.0 ± 2.2
22	40.7 ± 4.7	46.5 ± 1.7	19.8 ± 1.8	9.4 ± 0.4	>50
23	–	–	–	–	–
24	20.6 ± 0.6	50.1 ± 0.8	38.5 ± 0.7	40.8 ± 1.9	–
ADM	0.57 ± 0.32	0.46 ± 0.63	0.72 ± 0.12	0.48 ± 0.06	–

^aInactive at $100 \mu\text{M}$ (highest concentration tested).

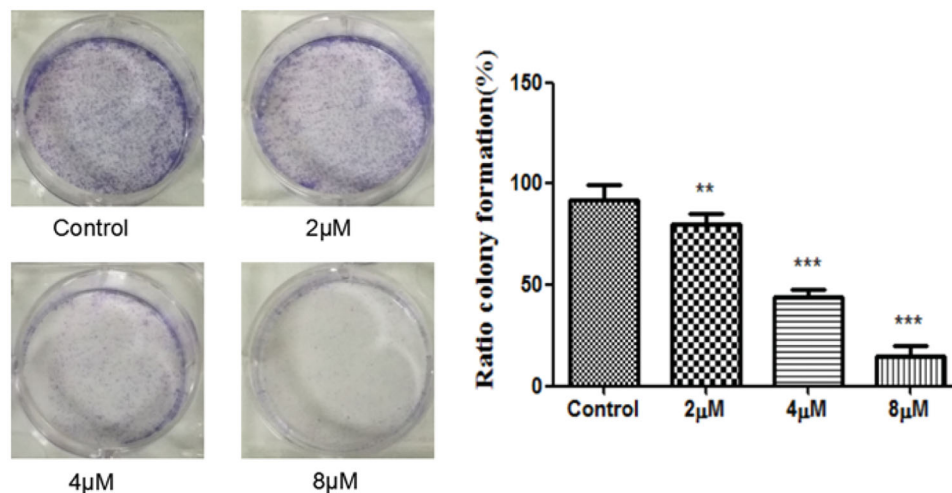


Figure 4. The SGC-7901 cells formed colonies (counted with Image-ProPlus) after treated with various concentrations of the compound **12** for 12 d. ** $p < 0.01$, *** $p < 0.001$ compared with the control group.

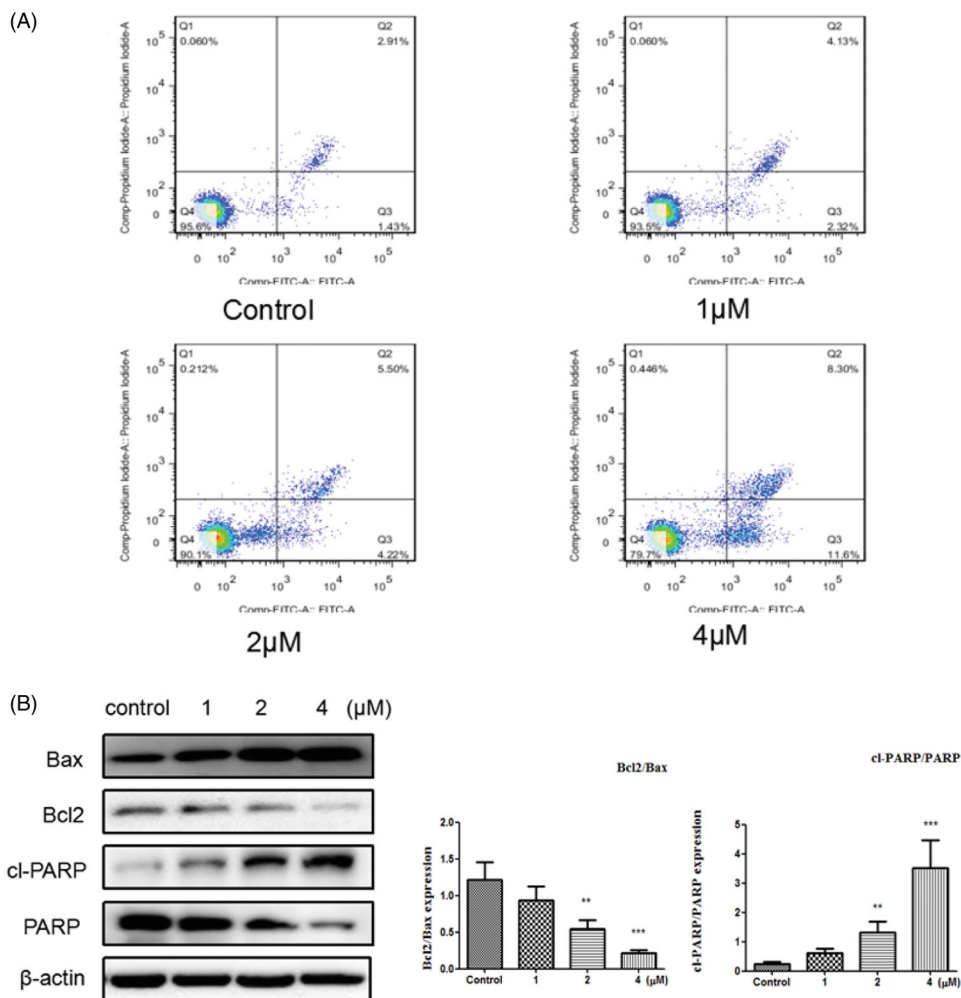


Figure 5. (A) Apoptosis ratio was detected by Annexin V/PI staining on the SGC-7901 cells treated with various concentration of title compound **12** (1, 2, 4 μM). (B) Western blots were used to detect the Bax, Bcl-2, cleaved PARP and full length PARP protein expression. *** $p < 0.001$, ** $p < 0.01$ compared with the control group.

Parent Remaining of compound **12** in metabolic stability test were 100, 95, 85, 80, and 70 at 0, 15, 30, 45, and 60 min, respectively. The calculated clearance rate was $>110 \mu\text{L}/\text{min}/\text{mg}$ and the half-life ($t_{1/2}$) was more than 60 min which indicated the acceptable stability.

3.5. Induces apoptosis

Apoptosis is one of the main methods that result in cell death^{37–39}. In this study, Annexin V-FITC/PI kit was used to evaluate the cell apoptosis. From **Figure 5(A)**, it can be seen that after the cells were treated with the compound **12** (1, 2, and 4 μM) for 48 h, the total apoptosis was increased to 6.45%, 9.72%, and 19.9%, respectively, compared to the control group (4.34%). These results indicated that compound **12** induced apoptosis was associated with a dose dependent. To further, investigate whether the cell apoptosis induced by title compound, Western blot analysis was used to measure the effect of the compound on apoptosis of SGC-7901 cell. As reported that apoptosis pathway could be regulated by the activation of PARP and Bcl2 family proteins^{40,41}. It can be found that the levels of Bax and cleaved PARP were up-regulated and the level of Bcl2 was down-regulated by the increased concentration of compound **12**, which suggested that compound could promote apoptosis in SGC-7901 cells (**Figure 5(B)**).

3.6. Induces autophagy

Autophagy is a process of lysosomal degradation that can deliver the cytoplasmic cargo to the lysosome⁴². To assess whether compound **12** could promote autophagy on SGC-7901 cells, the expressions of autophagy-related proteins were examined. Autophagy will be switched on when LC3-I was converted into LC3-II, and the level of LC3-II involves in the formation of autophagosome. Meanwhile p62 is a marker of the degradative lysosome^{43,44}. As shown in **Figure 6(A)**, compound can decrease the level of P62 and increase the expressions of LC3II and Beclin1. The preliminary results suggest that title compound may promote autophagy.

Another typical feature of autophagy is the accumulation of the acidic autophagic vacuoles (AVOs)^{45,46}. To verify the development of AVOs, Acridine Orange (AO) staining was used to examine whether the acidic vesicular organelles in SGC-7901 cells were increased. AO produces red fluorescence when it accumulates in acidic regions such as autophagy lysosomes and lysosomes and produces bright green fluorescence in the cytoplasm and the nucleus⁴⁷. As it can be seen in **Figure 6(B)**, red fluorescently labelled vesicle acidic accumulated obviously as the increased concentrations of title compound (1, 2, and 4 μM). GFP-LC3 indicating technique was also used to detect the autophagy at the same time. When autophagy is formed, multiple bright green fluorescent spots will form as the GFP-LC3 fusion protein can translate to autophagosome membrane⁴⁸. From **Figure 6(C)**,

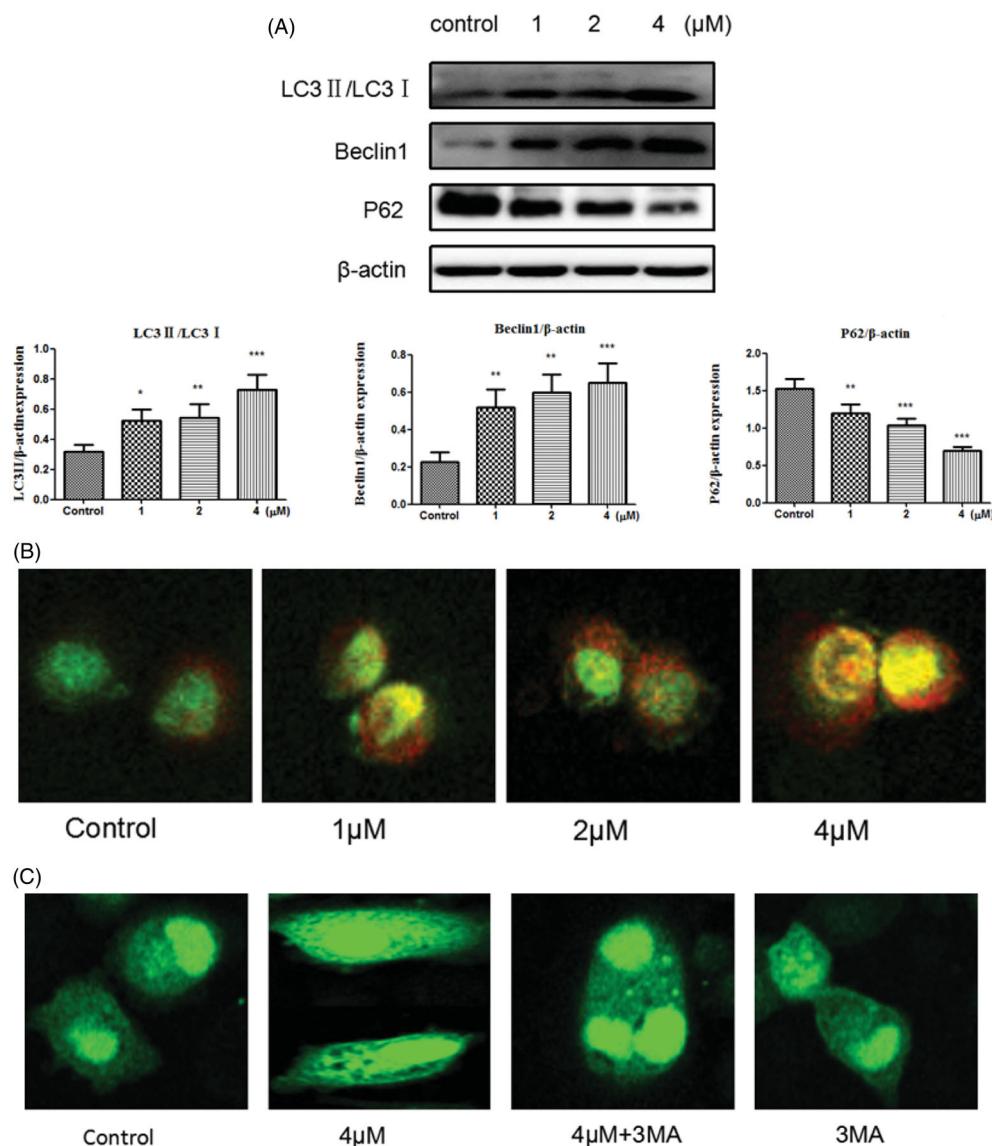


Figure 6. (A) Western blot assay examined the expressions of LC3-II/LC3-I, P62, Beclin1. * $p < 0.05$, ** $p < 0.01$, *** $p < 0.001$ compared with the control group. (B) SGC-7901 cells were stained with AO after exposed to compound 12 for 48 h, then detected by the confocal microscopy at 200 \times . (C) SGC-7901 cells were transfected with GFP-LC3 plasmid, and treated with compound 12 alone (4 μ M), 3MA (500 μ M, pre-incubated for 1 h), compound 12 and 3MA, then observed under a confocal microscopy at 200 \times .

compared to the blank control group, GFP-LC3 puncta were increased after cells treated with compound 12 (4 μ M) meanwhile decreased after treated with compound 12 (4 μ M) and 3-MA (500 μ M). This further proved that title compound can promote autophagy.

3.7. Role of autophagy regulation

The connection between apoptosis and autophagy is complicated because autophagy can promote apoptosis^{49,50}, and can also suppress apoptosis^{51,52}. To investigate whether autophagy has an impact on cell apoptosis induced by title compound, the cells were treated with compound 12 (4 μ M) for 48 h co-treatment with or absence of the 3-MA (500 μ M) in the apoptosis assays (Figure 7(A)) detected by the flow cytometry. Compared with compound 12, the apoptosis rate of treatment group cells in the presence of 3-MA decreased. At the same time, the levels of apoptosis-related proteins were examined in Western blot assay (Figure 7(B)), it was found that the up-regulation of apoptosis protein Bax and cl-PARP

and the down-regulation of Bcl-2 was inhibited in the group with 3-MA. These results indicated that cell autophagy induced by compound 12 might promote the apoptosis of SGC-7901 cells.

3.8. Suppression of activation of the PI3K/AKT/MTOR pathway

As a therapeutic target for cancer, the PI3K/AKT/MTOR signalling pathway participates in regulating autophagy⁵³⁻⁵⁶. Consequently, Western blot experiment was used to explore the impact of compound 12 on the level of phospho-PI3K, phospho-AKT and phospho-mTOR. After cells were treated with title compound for 48 h, the expression of p-PI3K, p-AKT and p-mTOR were decreased in a dose-dependent manner (Figure 8(A)). 3-MA (3-methyladenine) is also a PI3K inhibitor⁵⁷, so compound 12 (4 μ M) with 3-MA (500 μ M) were used to treat the cells. The experimental data showed that the ratio of p-PI3K/PI3K, p-AKT/AKT and p-mTOR/MTOR increased in the experiment of compound 12 with 3-MA compared with compound 12 alone (Figure 8(B)). These results revealed title compound could induce cell autophagy via inhibiting PI3K pathway.

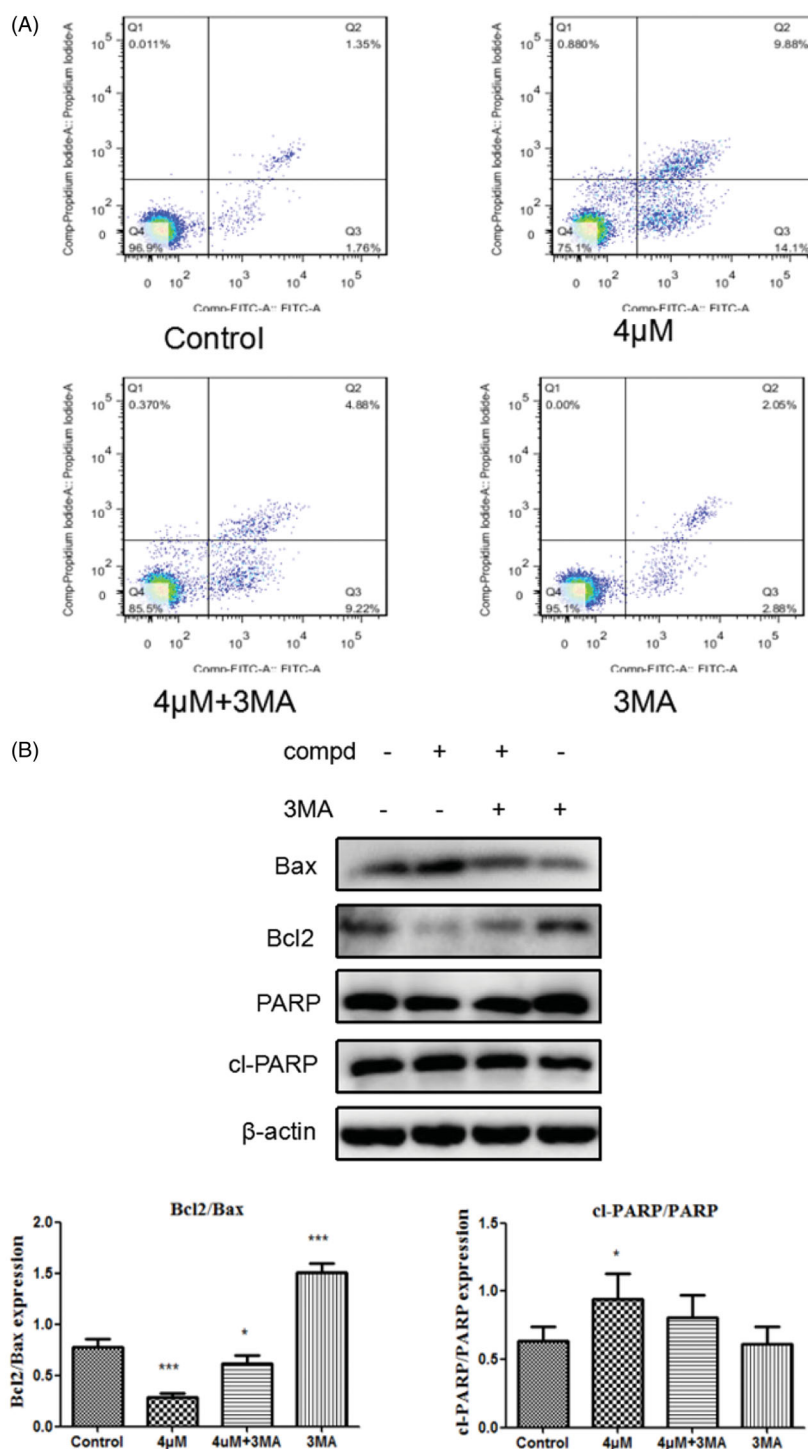


Figure 7. (A) Cells were treated with compound 12 alone (4 μ M), 3MA (500 μ M, pre-incubated for 1 h), compound 12 combined with 3MA and the Annexin-V-FITC staining was used to evaluate the apoptosis ratio. (B) The activation of Bax, Bcl2, cl-PARP were determined by the western blot after SGC-7901 cells were exposed to compound 12 for 48 h with or without of 3MA (500 μ M). * p < 0.05, *** p < 0.001 compared with the control group.

4. Conclusion

According to result of ligand profiler and docking, a series of naphthoquinone derivatives were designed and synthesised. The preliminary activity results showed that several compounds had good anticancer activity. The anticancer mechanism of one compound against SGC-7901 cells was investigated further. The expression of LC3-II and Beclin1 increased and the expression of P62 decreased after treated with this compound, which means that this compound helps promote the cell autophagy. Moreover,

in Western blot and GFP-LC3 studies, the level of LC3-II/LC3-I decreased and autophagosome puncta was reduced after pre-treatment with 3-MA, which further verify our view. In addition, the cell apoptosis induced by this compound was inhibited and the cell viability was increased when the cell autophagy was blocked by 3-MA. Sequentially, the levels of p-MTOR, p-AKT, and p-PI3K were suppressed after incubated with compound, and these indicated that title compound could negatively regulate the PI3K pathways. In conclusion, title compound could inhibit cancer cell growth by promoting autophagy.

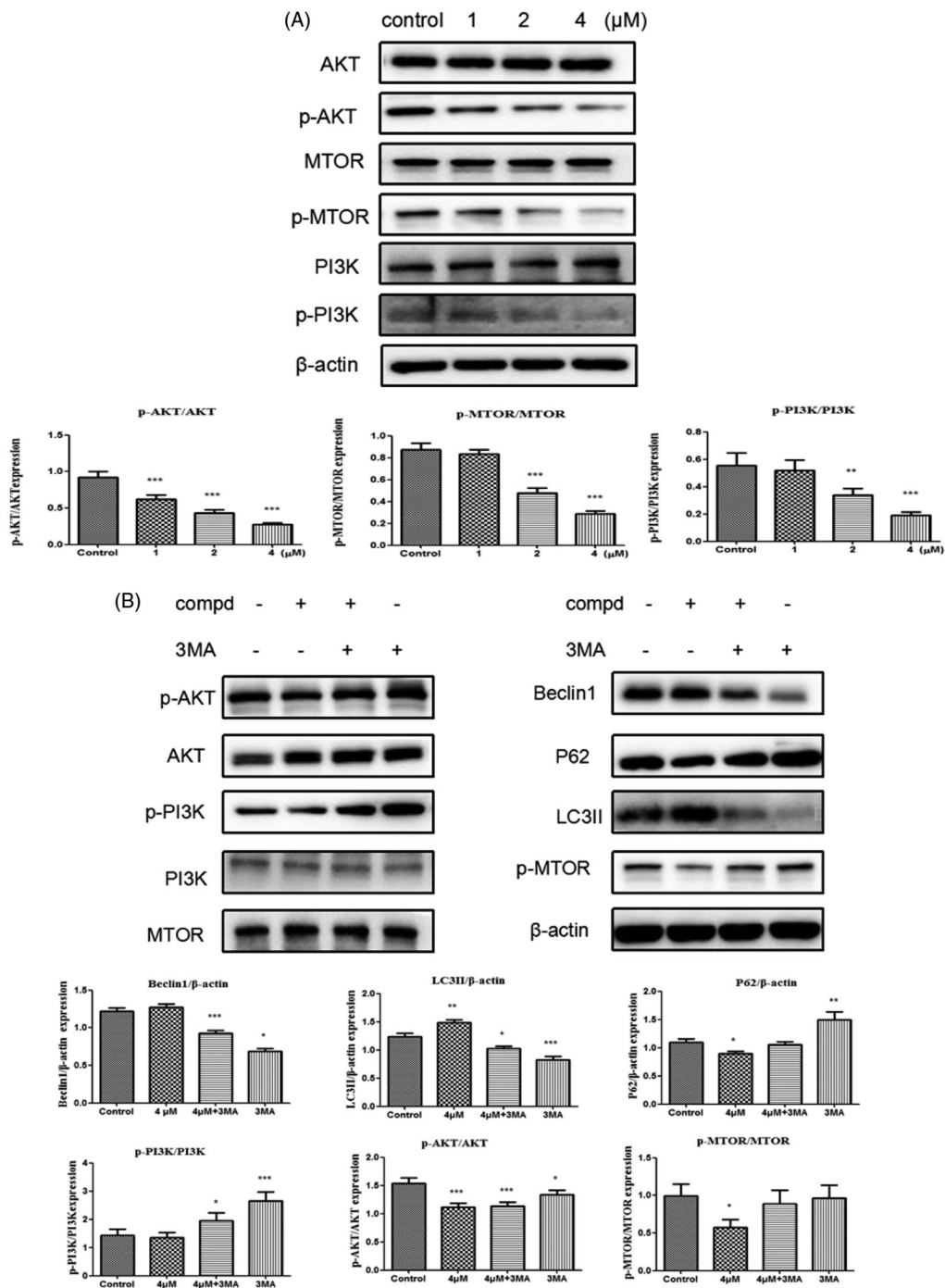


Figure 8. (A) Western blots were performed to observe the PI3K, p-PI3K, AKT, p-AKT, mTOR, p-mTOR protein expression incubated with compound 12 (1 μ M, 2 μ M, 4 μ M) for 48 h. * $p < 0.05$, ** $p < 0.01$, *** $p < 0.001$ compared with the control group. (B) The expression levels of LC3-II, Beclin-1, P62 and PI3K signalling were analysed by western blotting assay with or without pre-treatment of 3MA (500 μ M). * $p < 0.05$, *** $p < 0.001$ compared with the control group.

Disclosure statement

No potential conflict of interest was reported by the author(s).

[HX2019033], and Technological Fund of Fuyang normal university [2017FSKJ16].

Funding

The authors thank the National Natural Science Foundation of China [Nos. 21977001 and 21602029], the Horizontal cooperation project of Fuyang municipal government [Nos. XDHX201722 and XDHX2016026], Anhui Province Foundation [No. 18030701213], Horizontal cooperation project of Yifan Pharmaceutical Co., Ltd

References

1. Zhao TT, Xu H, Xu HM, et al. The efficacy and safety of targeted therapy with or without chemotherapy in advanced gastric cancer treatment: a network meta-analysis of well-designed randomized controlled trials. *Gastric Cancer* 2018; 21:361–71.

2. Ferlay J, Soerjomataram I, Dikshit R, et al. Cancer incidence and mortality worldwide: sources, methods and major patterns in GLOBOCAN 2012. *Int J Cancer* 2015;136:E359–86.
3. Levine B, Kroemer G. Autophagy in the pathogenesis of disease. *Cell* 2008;132:27–42.
4. Cao Y, Luo Y, Zou J, et al. Autophagy and its role in gastric cancer. *Clin Chim Acta* 2019;489:10–20.
5. Satyavarapu EM, Das R, Mandal C, et al. Autophagy-independent induction of LC3B through oxidative stress reveals its non-canonical role in anoikis of ovarian cancer cells. *Cell Death Dis* 2018;9:934.
6. Eisenberg-Lerner A, Bialik S, H-U S, et al. Life and death partners: apoptosis, autophagy and the cross-talk between them. *Cell Death Differ* 2009;16:966.
7. Meng Y, Yong Y, Yang G, et al. Autophagy alleviates neurodegeneration caused by mild impairment of oxidative metabolism. *J Neurochem* 2013;126:805–18.
8. Y Ávalos, Canales J, Bravo-Sagua R, et al. Tumor suppression and promotion by autophagy. *Biomed Res Int* 2014;2014:603980.
9. Castaño-Rodríguez N, Kaakoush NO, Goh KL, et al. Autophagy in *Helicobacter pylori* infection and related gastric cancer. *Helicobacter* 2015;20:353–69.
10. Burada F, Plantinga TS, Ioana M, et al. IRGM gene polymorphisms and risk of gastric cancer. *J Dig Dis* 2012;13:360–5.
11. Du W, Hao X, Yuan Z, et al. Shikonin potentiates paclitaxel antitumor efficacy in esophageal cancer cells via the apoptotic pathway. *Oncol Lett* 2019;18:3195–201.
12. Liu B, Jin J, Zhang Z, et al. Shikonin exerts antitumor activity by causing mitochondrial dysfunction in hepatocellular carcinoma through PKM2–AMPK–PGC1 α signaling pathway. *Biochem Cell Biol* 2019;97:397–405.
13. Li B, Yuan Z, Jiang J, et al. Anti-tumor activity of Shikonin against afatinib resistant non-small cell lung cancer via negative regulation of PI3K/Akt signaling pathway. *Biosci Rep* 2018;38:1–9.
14. Liu JP, Liu D, Gu JF, et al. Shikonin inhibits the cell viability, adhesion, invasion and migration of the human gastric cancer cell line MGC-803 via the Toll-like receptor 2/nuclear factor-kappa B pathway. *J Pharm Pharmacol* 2015;67:1143–55.
15. Papageorgiou VP, Assimopoulou AN, Couladouros EA, et al. The chemistry and biology of alkannin, shikonin, and related naphthazarin natural products. *Angew Chem Int Ed* 1999;38:270–301.
16. Deng B, Feng Y, Deng B. TIPE2 mediates the suppressive effects of shikonin on MMP13 in osteosarcoma cells. *Cell Physiol Biochem Int J Exp Cell Physiol Biochem Pharmacol* 2015;37:2434.
17. Andújar I, Ríos JL, Giner RM, et al. Shikonin promotes intestinal wound healing in vitro via induction of TGF- β release in IEC-18 cells. *Eur J Pharm Sci* 2013;49:637–41.
18. Liu Y, Kang X, Niu G, et al. Shikonin induces apoptosis and pro-survival autophagy in human melanoma A375 cells via ROS-mediated ER stress and p38 pathways. *Artif Cells Nanomed Biotechnol* 2019;47:626–35.
19. Gong K, Zhang Z, Chen Y, et al. Extracellular signal-regulated kinase, receptor interacting protein, and reactive oxygen species regulate shikonin-induced autophagy in human hepatocellular carcinoma. *Eur J Pharmacol* 2014;738:142–52.
20. Liu T, Xu L, Wang C, et al. Alleviation of hepatic fibrosis and autophagy via inhibition of transforming growth factor- β 1/Smads pathway through shikonin. *J Gastroenterol Hepatol* 2018;34:263.
21. Kim HJ, Hwang KE, Park DS, et al. Shikonin-induced necroptosis is enhanced by the inhibition of autophagy in non-small cell lung cancer cells. *J Transl Med* 2017;15:123.
22. Shi S, Cao H. Shikonin promotes autophagy in BXPc-3 human pancreatic cancer cells through the PI3K/Akt signaling pathway. *Oncol Lett* 2014;8:1087–9.
23. Zhang X, Li J, Yu Y, et al. Shikonin controls the differentiation of CD4⁺CD25⁺ regulatory T cells by inhibiting AKT/mTOR pathway. *Inflammation* 2019;42:1215–27.
24. Zhang FY, Hu Y, Que ZY, et al. Shikonin inhibits the migration and invasion of human glioblastoma cells by targeting phosphorylated β -catenin and phosphorylated PI3K/Akt: a potential mechanism for the 8Anti-Glioma efficacy of a traditional Chinese herbal medicine. *Int J Mol Sci* 2015;16:23823–48.
25. Chen Y, Wang T, Du J, et al. The critical role of PTEN/PI3K/AKT signaling pathway in shikonin-induced apoptosis and proliferation inhibition of chronic myeloid leukemia. *Cell Physiol Biochem Int J Exp Cell Physiol Biochem Pharmacol* 2018;47:981–93.
26. Liu M, Zhao G, Zhang D, et al. Active fraction of clove induces apoptosis via PI3K/Akt/mTOR-mediated autophagy in human colorectal cancer HCT-116 cells. *Int J Oncol* 2018;53:1363–73.
27. Porta C, Paglino C, Mosca A. Targeting PI3K/Akt/mTOR signaling in cancer. *Front Oncol* 2014;4:64.
28. Xuan Y, Hu X. Naturally-occurring shikonin analogues – a class of necroptotic inducers that circumvent cancer drug resistance. *Cancer Lett* 2009;274:233–42.
29. Zhen R, Xin L, Wen Z, et al. Synthesis and antitumor activity of β -hydroxyisovalerylshikonin analogues. *Eur J Med Chem* 2011;46:3934–41.
30. Kong WY, Chen XF, Shi J, et al. Design and synthesis of fluoroacylshikonin as an anticancer agent. *Chirality* 2013;25:757–62.
31. Lin HY, Li ZK, Bai LF, et al. Synthesis of aryl dihydrothiazol acyl shikonin ester derivatives as anticancer agents through microtubule stabilization. *Biochem Pharmacol* 2015;96:93–106.
32. Kim Y, You YJ, Ahn BZ. Naphthazarin derivatives (VIII): synthesis, inhibitory effect on DNA topoisomerase-I, and anti-proliferative activity of 6-(1-acyloxyalkyl)-5,8-dimethoxy-1,4-naphthoquinones. *Archiv Der Pharmazie* 2001;334:318–22.
33. Sankawa U, Otsuka H, Kataoka Y, et al. Antitumor activity of shikonin, alkannin and their derivatives. II. X-ray analysis of cyclo-alkannin leucoacetate, tautomerism of alkannin and cyclo-alkannin and antitumor activity of alkannin derivatives. *Chem Pharm Bull* 1981;29:116–22.
34. Wang JQ, Wang X, Wang Y, et al. Novel curcumin analogue hybrids: synthesis and anticancer activity. *Eur J Med Chem* 2018;156:493–509.
35. Cheng X, Shi JB, Liu H, et al. Discovery of (4-bromophenyl)(3-hydroxy-4-methoxyphenyl)methanone through up-regulating hTERT induces cell apoptosis and ER stress. *Cell Death Dis* 2017;8:e3016.
36. Ke Y, Liang JJ, Hou RJ, et al. Synthesis and biological evaluation of novel Jiyuan Oridonin A-1,2,3-triazole-azole derivatives as antiproliferative agents. *Eur J Med Chem* 2018;157:1249–63.
37. Mahdjour S, Guardia JJ, Rodríguez-Serrano F, et al. Synthesis and antiproliferative activity of podocarpane and totarane derivatives. *Eur J Med Chem* 2018;158:863–73.

38. Shankar R, Chakravarti B, Singh US, et al. Synthesis and biological evaluation of 3,4,6-triaryl-2-pyranones as a potential new class of anti-breast cancer agents. *Bioorg Med Chem* 2009;17:3847–56.
39. Senwar KR, Sharma P, Reddy TS, et al. Spirooxindole-derived morpholine-fused-1,2,3-triazoles: design, synthesis, cytotoxicity and apoptosis inducing studies. *Eur J Med Chem* 2015;102:413–24.
40. Harris MH, Thompson CB. The role of the Bcl-2 family in the regulation of outer mitochondrial membrane permeability. *Cell Death Differ* 2000;7:1182–91.
41. Gillies LA, Kuwana T. Apoptosis regulation at the mitochondrial outer membrane. *J Cell Biochem* 2014;115:632–40.
42. Kim J, Kim YC, Fang C, et al. Differential regulation of distinct Vps34 complexes by AMPK in nutrient stress and autophagy. *Cell* 2013;152:290–303.
43. Kabeya Y, Mizushima N, Ueno T, et al. LC3, a mammalian homologue of yeast Apg8p, is localized in autophagosomal membranes after processing. *EMBO J* 2000;19:5720–8.
44. Mizushima N. Methods for monitoring autophagy. *Int J Biochem Cell Biol* 2004;36:2491–502.
45. Chen Y, Azad MB, Gibson SB. Methods for detecting autophagy and determining autophagy-induced cell death. *Can J Physiol Pharmacol* 2010;88:285–95.
46. Liu Q LW, Sheng L, Zou C, et al. Design, synthesis and biological evaluation of novel asperphenamate derivatives. *Eur J Med Chem* 2016;110:76–86.
47. Jiao YN, Wu LN, Xue D, et al. *Marsdenia tenacissima* extract induces apoptosis and suppresses autophagy through ERK activation in lung cancer cells. *Cancer Cell Int* 2018;18:149.
48. Yao D, Zhou Y, Zhu L, et al. Design, synthesis and structure-activity relationship studies of a focused library of pyrimidine moiety with anti-proliferative and anti-metastasis activities in triple negative breast cancer. *Eur J Med Chem* 2017;140:155–71.
49. Crighton D WS, Prey JO, Syed N, et al. DRAM, a p53-induced modulator of autophagy, is critical for apoptosis. *Cell* 2006;126:121–34.
50. Shi YH, Ding ZB, Zhou J, et al. Targeting autophagy enhances sorafenib lethality for hepatocellular carcinoma via ER stress-related apoptosis. *Autophagy* 2011;7:1159–72.
51. Shrivastava A, Kuzontkoski PM, Groopman JE, et al. Cannabidiol induces programmed cell death in breast cancer cells by coordinating the cross-talk between apoptosis and autophagy. *Mol Cancer Ther* 2011;10:1161–72.
52. Wang FY, Xiao-Ming T, Xia W, et al. Mitochondria-targeted platinum(II) complexes induce apoptosis-dependent autophagic cell death mediated by ER-stress in A549 cancer cells. *Eur J Med Chem* 2018;155:639–50.
53. Avan A, Hassanian SM, Ghayour-Mobarhan M, et al. Targeting the Akt/PI3K signaling pathway as a potential therapeutic strategy for the treatment of pancreatic cancer. *Curr Med Chem* 2017;24:1321–31.
54. Kumar S GS, Pathania AS, Manda S, et al. Fascaplysin induces caspase mediated crosstalk between apoptosis and autophagy through the inhibition of PI3K/AKT/mTOR signaling cascade in human leukemia HL-60 cells. *J Cell Biochem* 2015;116:985–97.
55. Roy B, Pattanaik AK, Das J, et al. Role of PI3K/Akt/mTOR and MEK/ERK pathway in Concanavalin A induced autophagy in HeLa cells. *Chem Biol Interact* 2014;210:96–102.
56. Janku F, McConkey DJ, Hong DS, et al. Autophagy as a target for anticancer therapy. *Nat Rev Clin Oncol* 2011;8:528–39.
57. Wu YT, Tan HL, Shui G, et al. Dual role of 3-methyladenine in modulation of autophagy via different temporal patterns of inhibition on class I and III phosphoinositide 3-kinase. *J Biol Chem* 2010;285:10850–61.